

J. SALOMON<sup>1,✉</sup>  
J.-C. DRAN<sup>1</sup>  
T. GUILLOU<sup>1</sup>  
B. MOIGNARD<sup>1</sup>  
L. PICHON<sup>1</sup>  
P. WALTER<sup>1</sup>  
F. MATHIS<sup>2</sup>

# Ion-beam analysis for cultural heritage on the AGLAE facility: impact of PIXE/RBS combination

<sup>1</sup> Centre de Recherche et de Restauration des Musées de France, CNRS, UMR 171, Palais du Louvre, 14 Quai François Mitterrand, 75001 Paris, France

<sup>2</sup> Centre Européen d'Archéométrie, Institut de Physique Nucléaire, Atomique et de Spectroscopie, Université de Liège, Allée du 6 Août, bât. B15, 4000 Liège, Belgium

Received: 26 October 2007/Accepted: 15 January 2008  
Published online: 23 May 2008 • © Springer-Verlag 2008

**ABSTRACT** The combination of particle-induced X-ray emission (PIXE) and Rutherford backscattering (RBS) is particularly fruitful for the study of cultural heritage objects. Several set-ups have been developed at the AGLAE facility of the Louvre Laboratory to implement these techniques with an external beam. Successively have been tested the simultaneous use of PIXE and RBS with a single beam of protons, the sequential application of PIXE with protons and RBS with  $^4\text{He}^{2+}$  ions and finally the simultaneous implementation of PIXE and RBS with high-energy  $^4\text{He}^{2+}$  ions. Several examples illustrate the benefits of these combinations of techniques.

**PACS** 29.27.Eg; 29.30.Kv; 29.30.Ep

## 1 Introduction

Ion beam analysis (IBA) techniques are widely applied to many fields of research due to their remarkable analytical performances and their non-destructive character. Each field privileges a particular technique; for instance, Rutherford backscattering (RBS) is extensively used in materials science and particle-induced X-ray emission (PIXE) in earth and environmental sciences. Applications of IBA to cultural heritage also rely mainly on the use of PIXE because of its high sensitivity down to trace elements and its ease of implementation at atmospheric pressure [1]. However, PIXE has some limitations, namely its lack of depth information, which is frequently of primary importance in art works having multi-layered structure, such as paintings, glazed ceramics, bronzes with patina, etc. In contrast, RBS can provide detailed depth information but cannot be readily implemented in air, due to potential deterioration of the spectrum by the energy loss of the incident and scattered beams. We have attempted to combine the two techniques in order to take advantage of their complementary character. In particular, we have developed successive external-beam set-ups in order to improve the quality of the RBS mode, which is the critical factor of the whole set of measurements.

In the following sections, we first give a brief description of the different experimental set-ups and we illustrate

the progress made by giving examples of studies based on successively:

1. simultaneous PIXE/RBS analyses with a single proton beam;
2. sequential PIXE/RBS analyses respectively with two successive proton and alpha-particle beams;
3. simultaneous PIXE/RBS analyses with a single beam of high-energy  $^4\text{He}^{2+}$  ions.

## 2 Experimental set-ups for combined PIXE/RBS analyses

It is worth recalling the successive milestones which have led to the present sophisticated external-beam microprobe of the AGLAE facility.

After an early stage when IBA techniques were implemented in a conventional vacuum chamber, the necessity to operate in air soon became obvious, because most cultural heritage objects could not fit in the vacuum chamber nor stand the vacuum. We thus developed a first set-up for extracting a mm-sized proton beam through a window made of 8- $\mu\text{m}$  kapton foil, a material selected for its resistance to pressure and radiation damage (although one must note that hydrogen loss and graphitisation of the polymer cause changes both in the kapton thickness and in the beam stopping power) and for its low induced background [2]. However, it seemed to us that the only technique that could be used at atmospheric pressure was PIXE because it did not require beams of high quality in terms of energy definition.

The second step was the adjunction to the external beam line of the whole set of electromagnetic lenses (quadrupole triplet from Oxford Microprobe) that equipped a separate line under vacuum [3]. It was then possible to focus the beam down to 1  $\mu\text{m}$  on the vacuum side and thus to considerably reduce both the size and the thickness of the exit window. Indeed, we found in the market ultra-thin (0.1  $\mu\text{m}$ )  $\text{Si}_3\text{N}_4$  membranes (Silson, Northampton, UK) with remarkable properties: high mechanical strength and very low energy loss and angular straggling. As a consequence, the energy straggling of the external proton beam was so low that it became possible to carry out RBS measurements of the same quality as under vacuum. It should be noted that the scattering of protons in the MeV range is not ruled by the Rutherford law. However, for the sake of simplicity, we still label this analytical method as RBS. The layout of the set-up is shown in Fig. 1. Details of

✉ E-mail: joseph.salomon@culture.gouv.fr

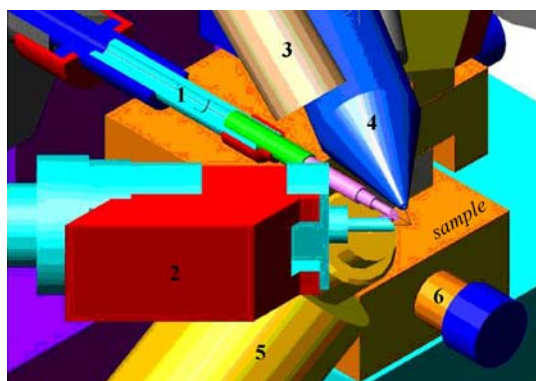


**FIGURE 1** Layout of the external microbeam set-up permitting simultaneous or sequential PIXE/RBS combination. 1: Beam extractor with  $\text{Si}_3\text{N}_4$  membrane mounted. 2: Low-energy X-ray detector equipped with a permanent magnet for backscattered particle removal. 3: High-energy X-ray detector equipped with a filter. 4: Surface barrier detector housing (under vacuum) for RBS measurements. A  $\text{Si}_3\text{N}_4$  membrane permits the collection of the RBS particles from the target. 5: Peltier detector for dose monitoring. 6: XYZ mechanical stage for precise positioning of item 4

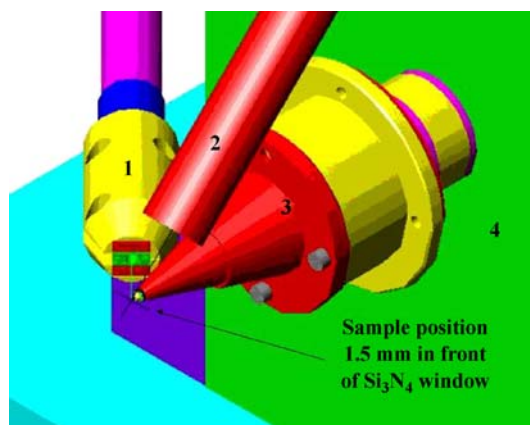


**FIGURE 2** Layout of the third-generation microbeam set-up permitting simultaneous or sequential PIXE/RBS combination with improved dose monitoring. 1: Low-energy X-ray detector equipped with a new permanent magnet for backscattered particle removal. 2: High-energy X-ray detector equipped with a filter. 3: Particle-collection cone, containing the surface-barrier detector. 4: Liquid-nitrogen cool trap for preventing (reducing) carbon deposition on the silicon nitride membrane

the role of the different components are given in previous articles [2, 3]. This system was well fitted to the simultaneous use of PIXE and RBS with protons of 3 MeV, the optimal energy for PIXE (high sensitivity and low background from nuclear reactions). We soon found that it was possible to extract beams of  $^4\text{He}^{2+}$  ions as well. The set-up was thus used for sequential combination of PIXE with protons and RBS with  $^4\text{He}^{2+}$  ions.

For obvious reasons, sequential PIXE/RBS is a very tedious approach and does not guarantee to analyse the same spot on the sample. Moreover, it implies twice the irradiation dose, which is not advisable for precious objects. These considerations led us to design a third-generation set-up that permits the simultaneous use of PIXE and RBS with 6-MeV  $^4\text{He}^{2+}$  ions, this high energy (maximum attainable with our tandem accelerator at the Louvre) being needed to ionise low-

to intermediate-Z elements. The layout is presented in Fig. 2. The main features are the following:

- the exit nozzle houses an annular surface barrier detector;
- this detector collects the RBS signal from the sample and is used for dose monitoring via a second RBS signal from a gold foil that is hit by the beam a fraction of the time via a beam-deflection system;
- the path of incident and backscattered particles takes place within a well-controlled helium atmosphere;
- the RBS geometry is markedly improved in terms of mass resolution, since the compactness of the set-up permits an angle of  $170^\circ$  for the detection of backscattered particles, whereas the previous set-up works at  $150^\circ$ ;
- the analysis of art works of complex shape is considerably facilitated due to this compactness.

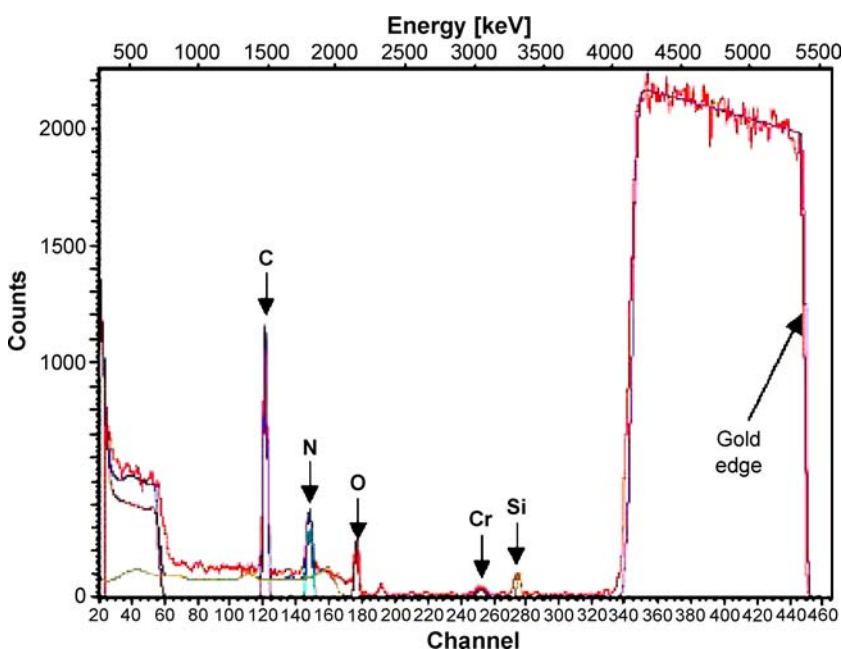


**FIGURE 3** Six MeV alpha RBS spectra (experimental and SIMNRA simulation) of the reference sample ( $2\text{-}\mu\text{m}$  Au on  $\text{SiO}_2$ ). In these spectra one can see the peaks due to the  $\text{Si}_3\text{N}_4$  membrane and also some carbon and oxygen due to bad vacuum

We recorded successive RBS spectra induced by 3-MeV proton beams of different intensities (1 to 4 nA) on a standard target and obtained a very good reproducibility for our monitoring experiment (variation less than 2%).

Figure 3 presents a RBS spectrum obtained on a standard made of a 2- $\mu\text{m}$ -thick gold layer deposited on a silica substrate. A very thin layer of chromium is inserted in between to enhance adhesion. The experimental spectrum was obtained with a 6-MeV alpha beam and the data simulated with the SIMNRA code. We can first notice a quite good agreement between them. We also note the peaks corresponding to silicon and nitrogen coming from the exit window, and the two peaks corresponding to carbon and oxygen without energy loss, which are in fact experimental artefacts coming from hydrocarbons present in our beam line and deposited on the window by the ion beam.

### 3 Simultaneous PIXE/RBS analyses with a single proton beam

As already stated, the first external-beam set-up fixed to the AGLAE accelerator was restricted to the PIXE mode. It was very soon equipped with a RBS attachment to collect the backscattered protons. Combining PIXE and RBS with a single proton shot offers the obvious advantage of a short measurement time and of analysed areas in both modes that are strictly identical. In addition, the long range of incident protons permits us to analyse a large thickness of material, a feature which can be appropriate to the study of materials having a thick alteration layer. Although RBS with protons can be sometimes useful, it suffers from poor mass and depth resolution and also from the relative difficulty to quantify the data in comparison to true RBS measurement with  $^4\text{He}^{2+}$  ions. Nevertheless, the existence of well-described resonances for light elements like B, C, O or Si often allows depth-distribution determination. We illustrate the capability of such a PIXE/RBS combination by two examples.

#### 3.1 Russian icons (Fig. 4)

Several Russian icons were studied with the aim to check their authenticity [4]. The icon gilds are composed of gold and silver foils or of alloys of these two metals. Figure 5 displays a PIXE spectrum showing clearly the characteristic X-ray peaks of gold (mainly LX rays) and of silver (mainly KX rays) as well as those of other elements such as Fe, Ca and Pb, which are the constituents of pigments. Figure 6 shows the corresponding RBS spectrum whereas Fig. 7 concerns the analysis of another icon where these two elements are completely absent, the golden aspect being generated by the presence of a 2- $\mu\text{m}$ -thick layer containing aluminium powder mixed with an organic binder. One can also observe the presence of many elements such as C, O and heavier Si, Fe, Pb present in the decoration pigments such as, for example, the red ochre ( $\text{Fe}_2\text{O}_3$ ), the yellow iron oxide, the  $\text{PbCrO}_4$  chromium yellow or the lead white. All these spectra have been processed using the SIMNRA computer code version 5.0 [5]. This code simulates a spectrum by superposition of discrete layers whose composition and thicknesses are adjusted to identify the simulated spectrum with the experimental spectrum. This data processing clearly shows the



FIGURE 4 Picture of a Russian icon

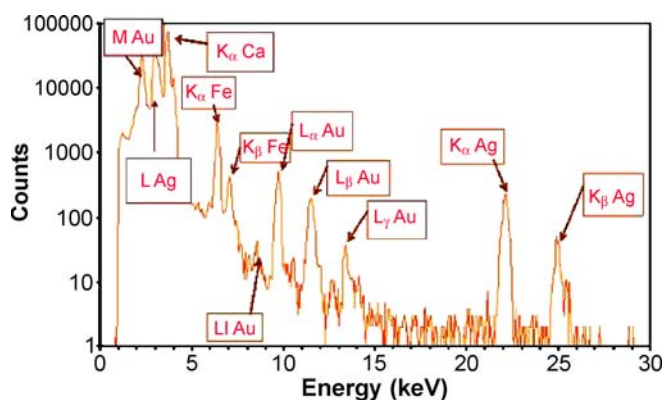


FIGURE 5 Composition identification of the gilded parts of a Russian icon by means of 3-MeV proton PIXE

excellent complementarity of the PIXE and RBS techniques in this field of applications.

#### 3.2 Gilded bronze components of the chandelier of the Hildesheim cathedral, Germany

The bronze chandelier of the Hildesheim cathedral (Fig. 8) was created between 1055 and 1065 AD. It has been heavily modified and restored in the past. Parts of the chandelier were displayed in Paris during an exhibition and on this occasion brought to our laboratory for investigation. In particular, we have performed a study of the gilded surfaces by ion beam analysis techniques [6]. The aim is to bring to the restorers as much information as possible to guide their restoration program.

PIXE analysis of the gilded regions (Fig. 9) brings only qualitative results, because the obtained composition is averaged over the penetration of the proton beam. The most interesting results are that the surface layer always contains a noticeable amount of silver and the original parts contain only mercury. This shows that the original parts have been gilded by the mercury process (fire gilding) and the restored parts by the electrolytic process. The metal used for both processes is a gold–silver–(possibly copper) alloy. Using the quantitative analysis GUPIX code in the multiple-layer mode,

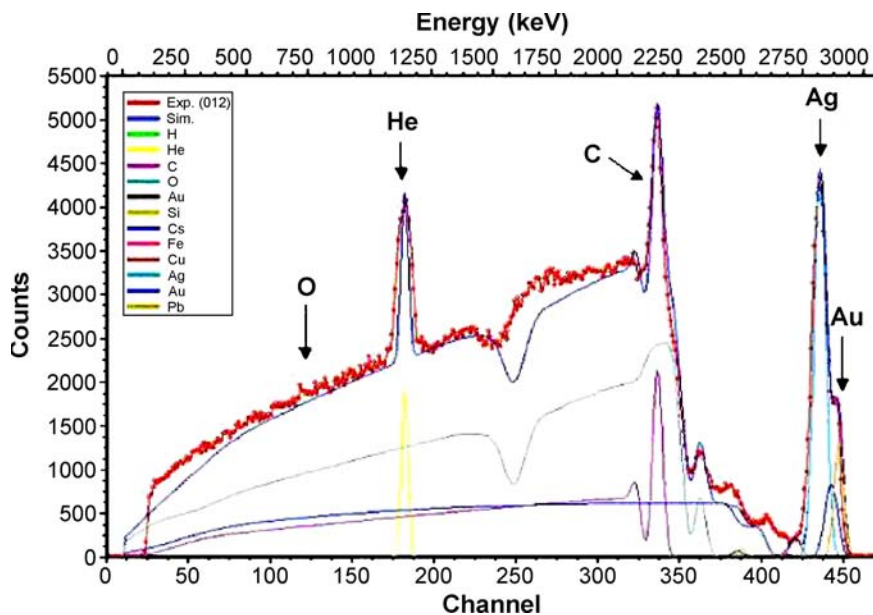


FIGURE 6 RBS spectrum with 3-MeV protons obtained on the same icon as in Fig. 5. Discrimination between Ag–Au bilayer and alloy

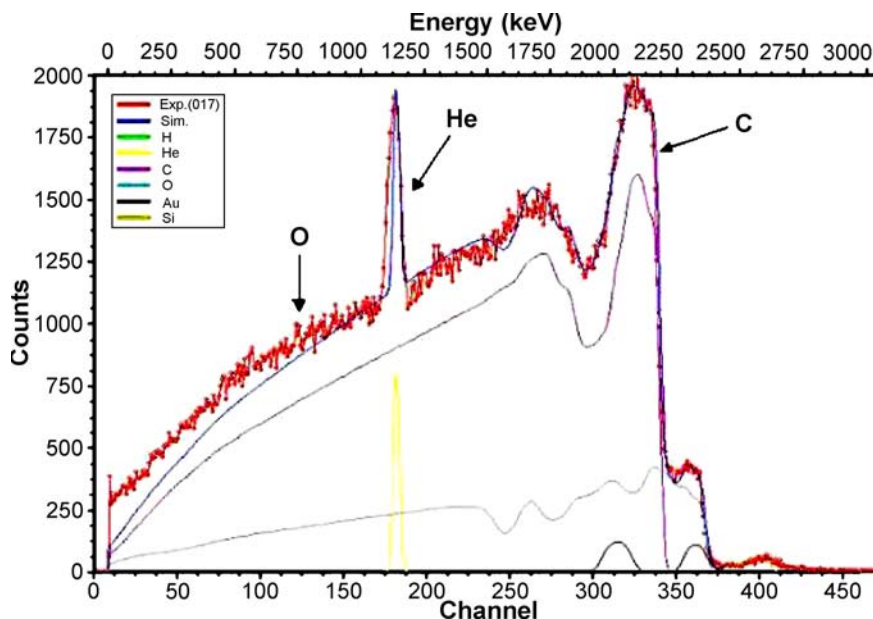


FIGURE 7 RBS spectrum with 3-MeV protons obtained with another icon which does not contain either gold or silver

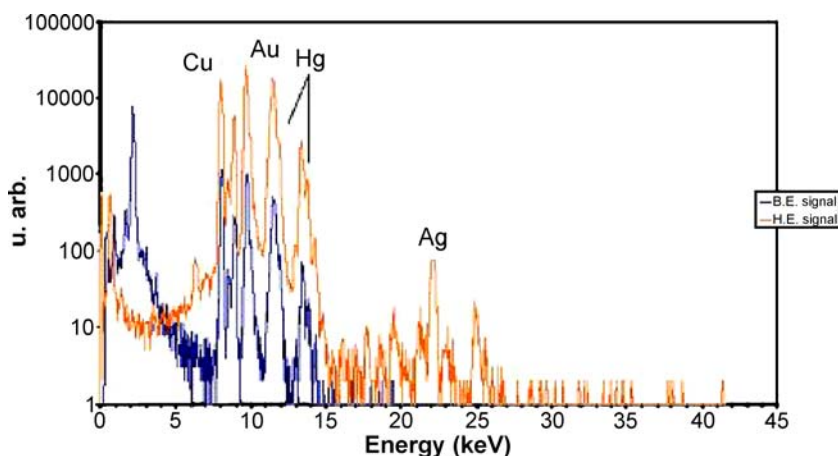
the gold content in the surface gilding film is estimated to be less than 85 wt. %.

Several RBS spectra have been obtained on various regions either in the original parts or in the restored parts. The results may be summarised as follows:

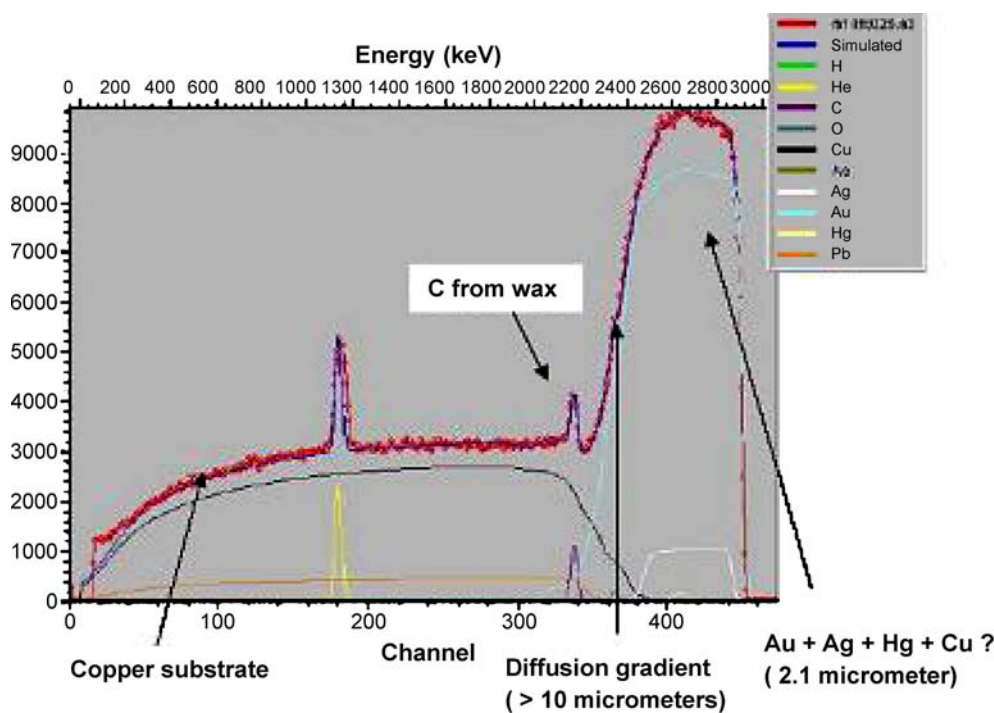
- a wax or varnish layer has been applied to the surface, presumably during restoration. Some sources indicate that this may be a beeswax application;
- the mercury original gilding (Fig. 10) is indeed a fire gilding using mercury amalgam and an Au–Ag alloy (possibly containing some Cu) of less than 85 wt. % Au content ( $\sim 20$  carats). The thickness of the gold film is large (several  $\mu\text{m}$ ) but strongly inhomogeneous. Fire gilding has induced a noticeable diffusion of gold (and silver) into the substrate over a distance larger than  $10\ \mu\text{m}$  from the interface;



FIGURE 8 The bronze chandelier of the Hildesheim cathedral (a 6-m-diameter ‘Crown of light’ figuring the celestial Jerusalem)



**FIGURE 9** Typical set of PIXE spectra (low-energy and high-energy detectors) of a gilded component of the chandelier



**FIGURE 10** RBS spectrum with 3-MeV protons of an original gilded part of the chandelier

- the electrolytic restoration gilding (Fig. 11) has been done by using an anode of the same composition as the original gilding (85 wt. % Au alloy), presumably in order to obtain the same coloured aspect as the original gilding. The gold film is thin (less than 0.5  $\mu\text{m}$ ) and not homogeneous. The electrolytic process results in the occurrence of an intermediate hydrogen-containing layer between the surface gold film and the substrate. No gold diffusion has occurred into the substrate.

#### 4 Sequential PIXE/RBS analyses with protons and $^4\text{He}^{2+}$ ions

In the framework of the Eu-ARTECH European project, a large collection of glazed ceramics was investigated with special interest in the lustre technology (Fig. 12). The objective is to understand the stepwise evolution of this technology initiated in the Middle East in the 9th century and progressively diffused in Europe via North Africa and Spain.

Several prestigious plates from Gubbio workshops have been brought to our laboratory for analysis combining PIXE with 3-MeV protons followed by RBS with 3-MeV  $^4\text{He}^{2+}$  ions [7].

A typical set of PIXE spectra is shown in Fig. 13. We recall that the lustre is made of an heterogeneous layer of glaze of a few hundred nanometres containing silver and/or copper nanometric clusters. Such an heterogeneity makes difficult the quantification of PIXE, which therefore is only used to identify the components present in the glaze.

The corresponding RBS spectrum obtained with 3-MeV  $^4\text{He}^{2+}$  ions is presented in Fig. 14. Contrary to the elemental analysis by PIXE, RBS is poorly sensitive to light elements, but has a fairly good accuracy for the estimation of the metallic element contents and depth distributions. This means that the values given below for the thicknesses and Ag and Cu contents of the lustre layers are given with a good precision (5% for metal contents, less than 20 nm for thicknesses), whereas the precise compositions of the glassy matrix of the lustre and of the glazes are much more precisely obtained through

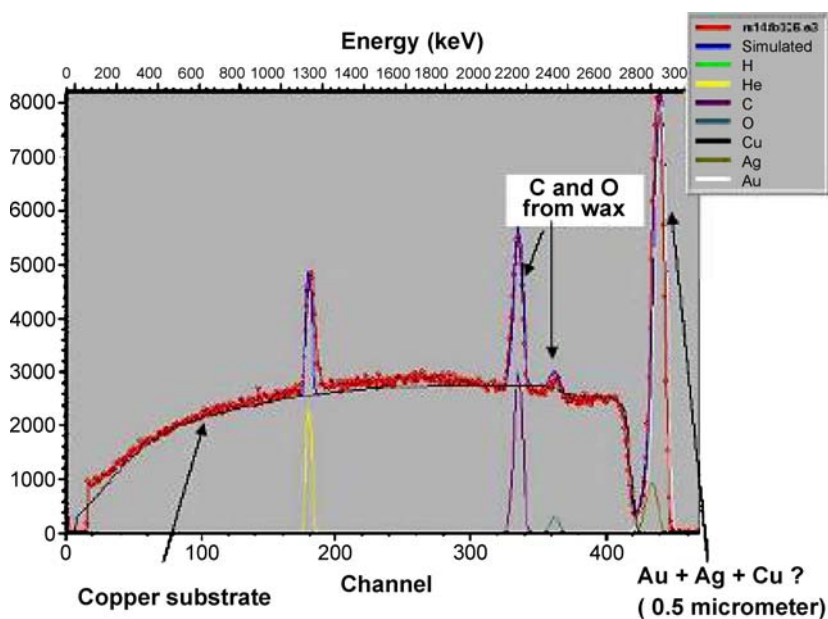


**FIGURE 11** RBS spectrum with 3-MeV protons of a restored gilded part of the chandelier



**FIGURE 12** Three examples of Renaissance glazed plates from the workshop of Mastro Giorgio of Gubbio, Italy

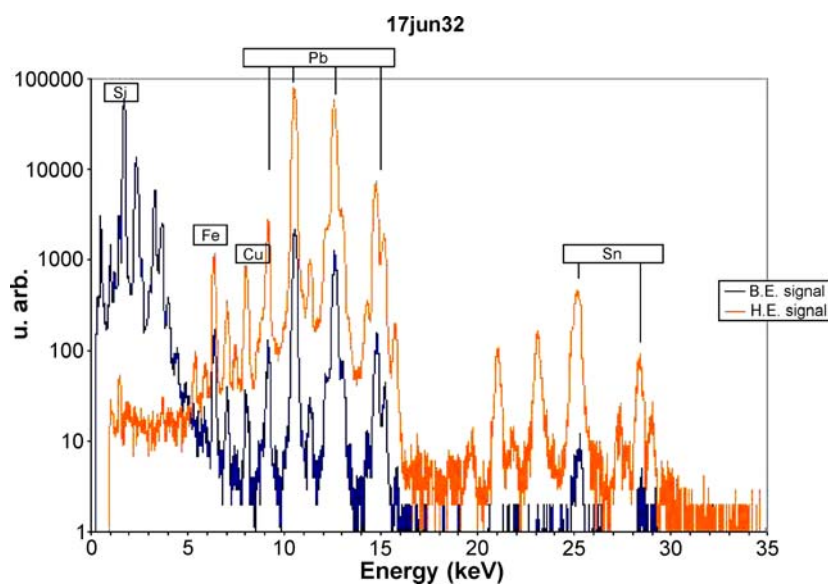


**FIGURE 13** PIXE spectra (low- and high-energy detectors) of a part of a ceramic with a lustre

	O at. %	Na at. %	Al at. %	Si at. %	K at. %	Ca at. %	Cu at. %	Ag at. %	Pb at. %	Thickness 10 <sup>15</sup> at./cm <sup>2</sup>	nm
Layer	62.0	1.7	1.5	30.1	3.3	0.6	0.0	0.0	0.5	550	77
Lustre	54.8	0.0	0.0	19.4	3.0	0.6	5.0	13.0	4.2	650	92
Glaze (PIXE)	62.0	1.7	1.5	25.1	3.3	0.6	0.0	0.0	5.5		

**TABLE 1** Values for different thicknesses and Ag, Cu contents of the lustre layers are given with a good precision (5% for metal contents, less than 20 nm for thicknesses). The precise composition of the glassy matrix of the lustre and of the glazes are much more precisely obtained through PIXE analyses

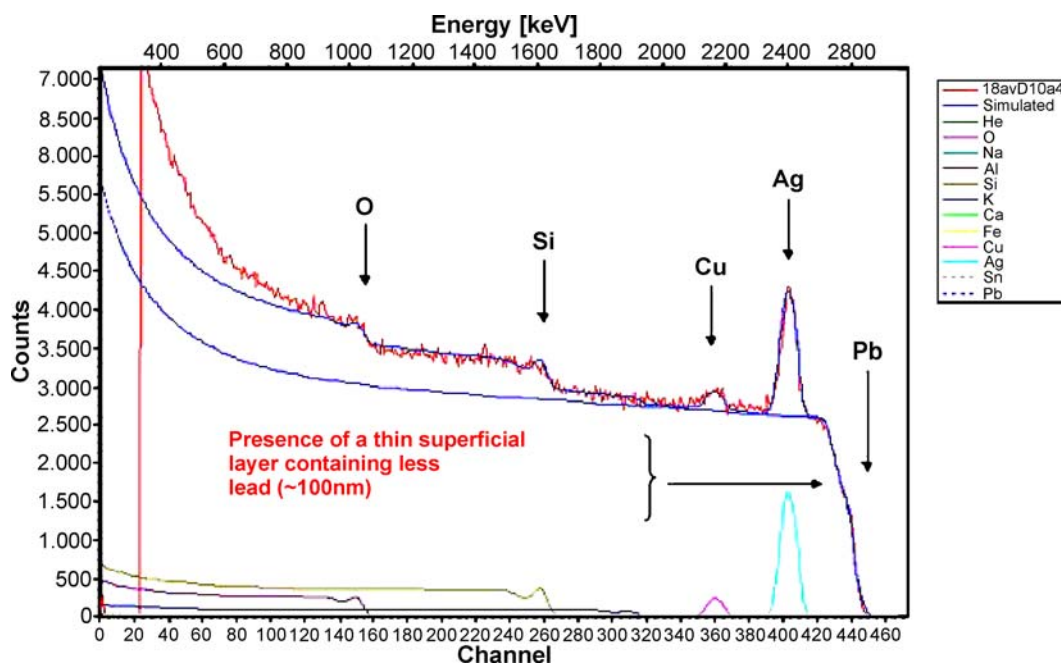


FIGURE 14 RBS spectrum with 3-MeV  $^4\text{He}^{2+}$  ions of the lustre zone of the same ceramic as in Fig. 13. The presence of a thin glass layer containing no lead is shown

PIXE analyses (Table 1). In fact, RBS is up to now the only non-destructive technique able to precisely provide the thickness and composition of metal-containing thin layers on lustre potteries.

## 5 Simultaneous PIXE/RBS analyses with a single beam of high-energy $^4\text{He}^{2+}$ ions

The last type of PIXE/RBS combination consists of the simultaneous implementation of these techniques using a high energy alpha particle beam. 6-MeV  $^4\text{He}^{2+}$  ions have higher stopping power than 3-MeV protons; they will mostly probe the first micrometres of the sample surface. On the other hand, their ionisation cross section (PIXE) becomes interesting at these energies (6 MeV and more). As a consequence, they are a good compromise for quality RBS measurements on a relatively large depth and reasonably good PIXE analysis at least for light and intermediate elements.

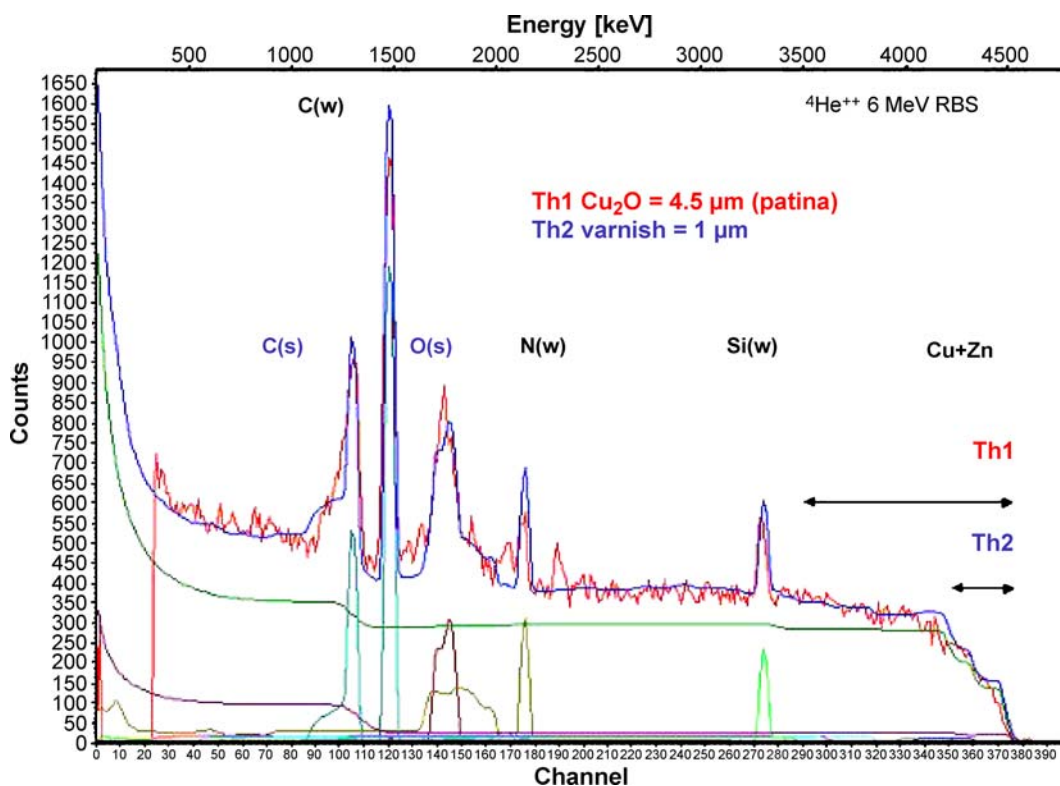


FIGURE 15 Picture of a Roman strigil. The patina of the handle is decorated with ivy leaves

High-energy  $^4\text{He}^{2+}$  ions could be well adapted to probe layers deposited on a substrate as well in RBS mode as in PIXE mode, without probing the bulk material: elemental analysis by PIXE will thus be more relevant. The interest of this approach is still under evaluation. Its first application was the study of a Roman strigil Fig. 15, a beauty care tool made of bronze [8]. The investigated object was found in the necropolis of the Roman colony of Sicca Veneria in Tunisia. This artefact has been first subjected to PIXE analysis with 3-MeV protons; the inferred copper to zinc ratio is very close to that of the alloy obtained by inductively coupled plasma-atomic emission spectrometry (ICP-AES) ( $\text{Cu}/\text{Zn} = 4.5$ ). The use of a 6-MeV alpha particle beam gives a higher ratio ( $\text{Cu}/\text{Zn} = 7.3$ ) showing a dezincification at the surface due to the normal corrosion of archaeological brass. The in-depth description of the patina by means of the RBS signal is also better with this beam, due to its better mass resolution and its lower penetration into the material. The RBS spectrum shown in Fig. 16 shows a 5.5- $\mu\text{m}$ -thick homogeneous patina (assuming a density close to the theoretical one) composed mainly of copper and oxygen with a ratio near that of cuprous oxide ( $\text{Cu}_2\text{O}$ ). The patina also contains chloride, as evidenced by the PIXE spectrum (not shown here), and is covered by a thin layer containing in majority carbon and oxygen, which can be attributed to a modern protective wax layer.

## 6 Conclusion and prospects

The development of a sophisticated external-beam set-up has permitted us to implement simultaneously or sequentially PIXE (particle induced gamma ray emission, PIGE) and RBS. The advantages and limitations of the three types of combination can be summarised as follows: the simultaneous use of PIXE and RBS with 3-MeV protons provides a fast analysis on the same spot, with a large depth for RBS measurement and the possibility to analyse light elements



**FIGURE 16** RBS spectrum with 6-MeV  $^4\text{He}^{2+}$  ions of a Roman strigil showing the thickness of the patina covered by a varnish layer. (s) Signal from the sample, (w) signal from the window

with the PIGE technique. The drawbacks are the poor mass and depth resolution of the RBS mode and the relatively difficult quantification in this mode, because the scattering cross sections are not accurately known (non-Rutherford regime).

- The sequential combination of PIXE (3-MeV protons) and RBS (3-MeV  $^4\text{He}^{2+}$  ions) offers the full capability of the PIXE/PIGE association, together with good mass and depth resolution and easy quantification in RBS mode. On the other hand, the analysis is longer, does not concern the same spot for PIXE and RBS and the depth accessible to RBS is smaller;
- the simultaneous implementation of PIXE and RBS with 6-MeV  $^4\text{He}^{2+}$  ions provides fast measurements on the same spot with good mass and depth resolution for RBS but with PIXE analysis limited to low- and intermediate-Z elements and no possibility of using the PIGE technique.

The third-generation set-up is currently under improvement to permit nuclear reaction analysis (NRA) measurement (depth profiles of light elements) in addition to PIXE and RBS. The coupling of all these techniques can provide a wealth of information on cultural heritage objects, not easily attainable with any other single method. Although X-ray fluorescence (XRF) (specially on synchrotron radiation lines) can be substituted

for PIXE for trace-element analysis, PIXE (and thus the whole set of IBA techniques) remains attractive because it can be complemented by PIGE for the measurements of light elements in the bulk material and RBS + NRA for depth profiling in the near-surface region.

**ACKNOWLEDGEMENTS** We thank M. Aucouturier, A. Bouquillon, Y. El Masri and F. Mathis for fruitful discussions.

## REFERENCES

- 1 J.-C. Dran, J. Salomon, T. Calligaro, P. Walter, Nucl. Instrum. Methods B **219–220**, 7 (2004)
- 2 T. Calligaro, J.D. MacArthur, J. Salomon, Nucl. Instrum. Methods B **109–110**, 125 (1996)
- 3 T. Calligaro, J.-C. Dran, H. Hamon, B. Moignard, J. Salomon, Nucl. Instrum. Methods B **136–138**, 339 (1998)
- 4 M. Morelle, Y. El Masri, C. Heitz, R. Prieels, J. Van Mol, J.-C. Dran, J. Salomon, T. Calligaro, M. Dubus, Nucl. Instrum. Methods B **204**, 600 (2005)
- 5 M. Mayes, SIMNRA user's guide, Tech. Rep. I PP 9/113, Max-Planck-Institut für Plasmaphysik, Garching, Germany (1997)
- 6 M. Aucouturier, A. Zyma, B. Mille, A. Texier, D. Bourgarit, in *Proc. Conf. Art 2002*, Antwerp, 2–6 June (2002)
- 7 G. Padeletti, G.M. Ingo, A. Bouquillon, S. Pages-Camagna, M. Aucouturier, S. Roehrs, P. Fermo, Appl. Phys. A **83**, 475 (2006)
- 8 F. Mathis, B. Moignard, L. Pichon, O. Dubreuil, J. Salomon, Nucl. Instrum. Methods B **240**, 532 (2005)